Constructing gravitational wave templates in extended gravity scenarios

Takahiro Tanaka

Kyoto University

Innovative Area (FY2017-2021) 科研費 KAKENHI

Gravitational Wave Physics and Astronomy : Genesis

Our Innovative Area (grant) has started in summer 2017.

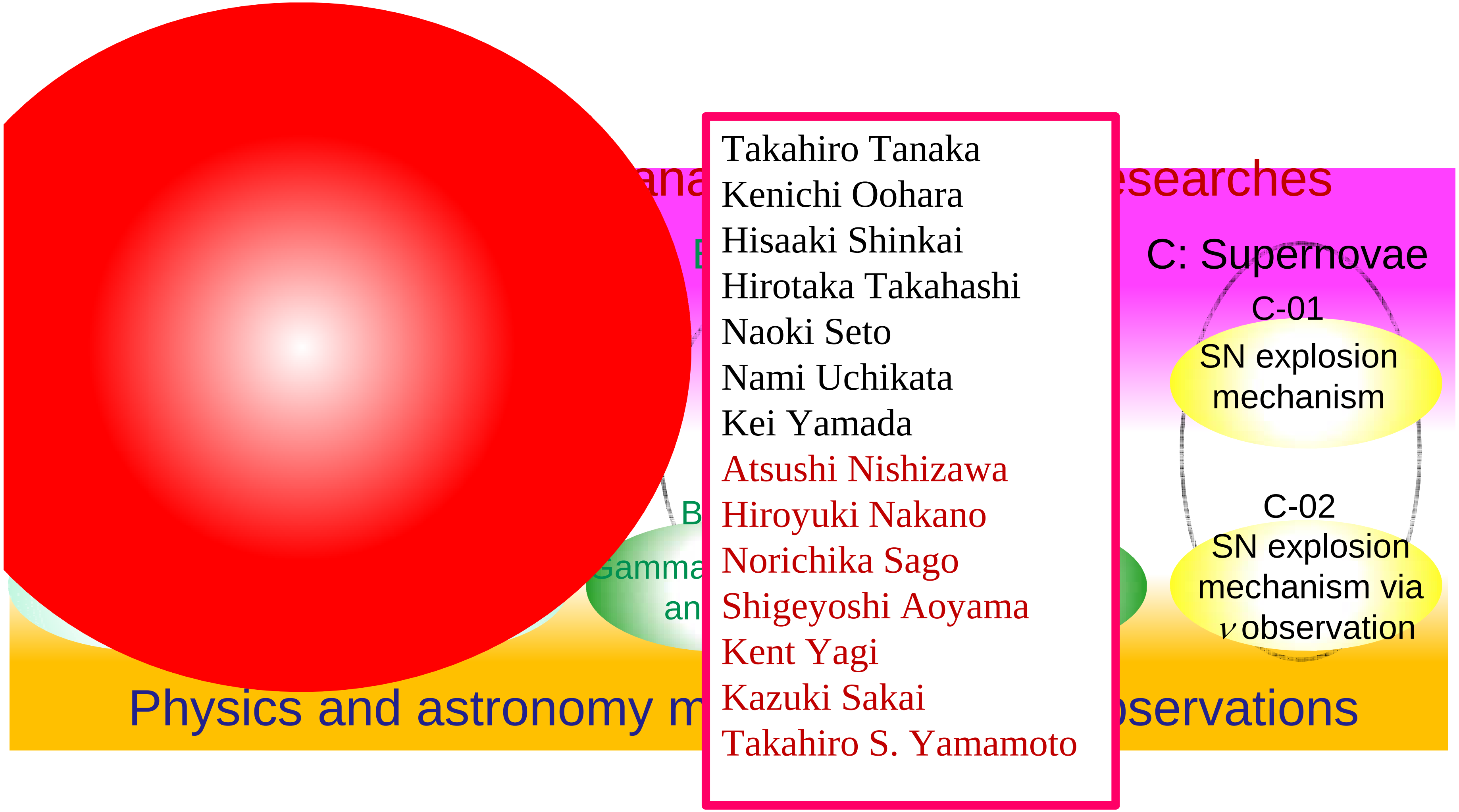

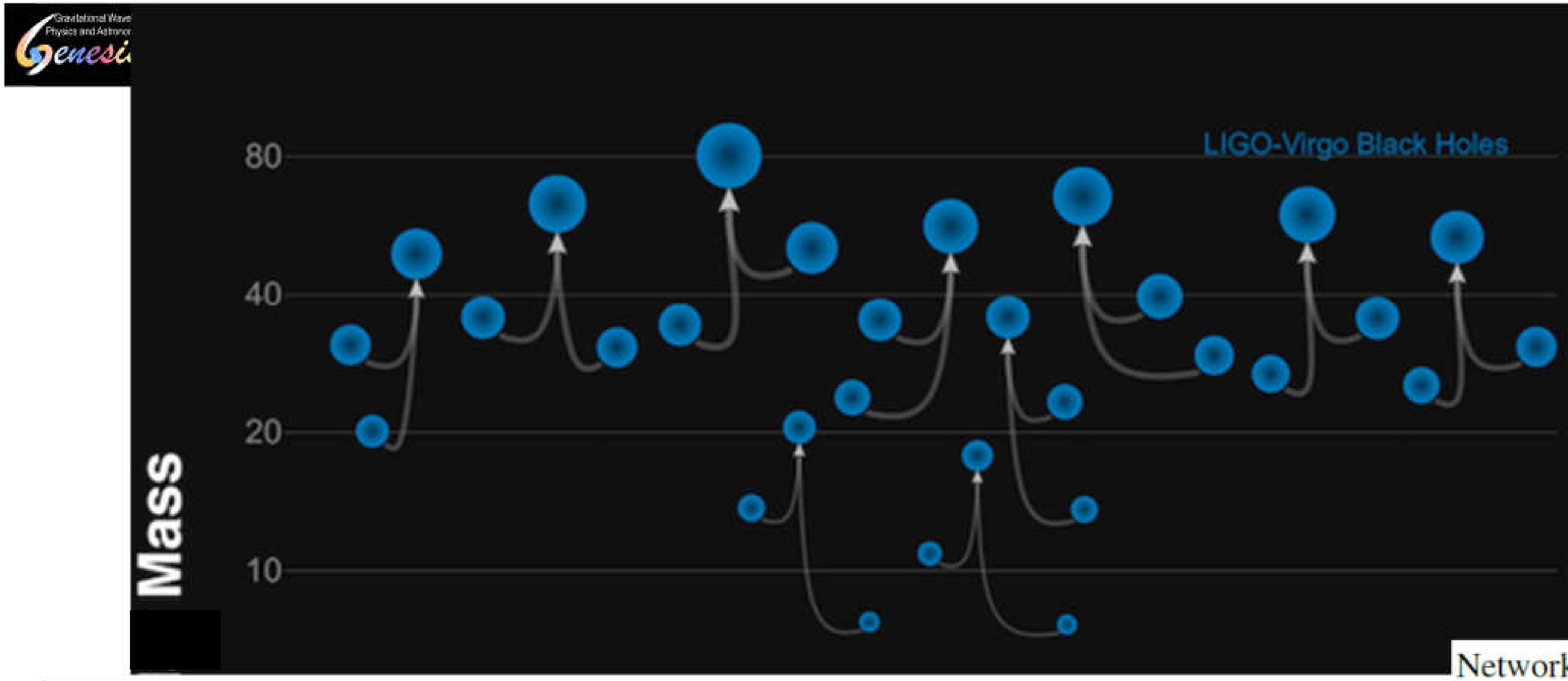

Event	$m_1/M_\odot$	$m_2/M_\odot$	$\mathcal{M}/M_\odot$	χ_{eff}	$M_f/M_\odot$	a_f	$E_{rad}/(M_\odot c^2)$	$\ell_{peak}/(erg\,s^{-1})$	d_L/Mpc	z	$\Delta\Omega/deg^2$	Network SNR GstLAL
GW150914	$35.6^{+4.8}_{-3.0}$	$30.6^{+3.0}_{-4.4}$	$28.6^{+1.6}_{-1.5}$	$-0.01^{+0.12}_{-0.13}$	$63.1^{+3.3}_{-3.0}$	$0.69^{+0.05}_{-0.04}$	$3.1^{+0.4}_{-0.4}$	$3.6^{+0.4}_{-0.4} \times 10^{56}$	430^{+150}_{-170}	$0.09^{+0.03}_{-0.03}$	179	24.4
GW151012	$23.3^{+14.0}_{-5.5}$	$13.6^{+4.1}_{-4.8}$	$15.2^{+2.0}_{-1.1}$	$0.04^{+0.28}_{-0.19}$	$35.7^{+9.9}_{-3.8}$	$0.67^{+0.13}_{-0.11}$	$1.5^{+0.5}_{-0.5}$	$3.2^{+0.8}_{-1.7} \times 10^{56}$	1060^{+540}_{-480}	$0.21^{+0.09}_{-0.09}$	1555	10.0
GW151226	$13.7^{+8.8}_{-3.2}$	$7.7^{+2.2}_{-2.6}$	$8.9^{+0.3}_{-0.3}$	$0.18^{+0.20}_{-0.12}$	$20.5^{+6.4}_{-1.5}$	$0.74^{+0.07}_{-0.05}$	$1.0^{+0.1}_{-0.2}$	$3.4^{+0.7}_{-1.7} \times 10^{56}$	440^{+180}_{-190}	$0.09^{+0.04}_{-0.04}$	1033	13.1
GW170104	$31.0^{+7.2}_{-5.6}$	$20.1^{+4.9}_{-4.5}$	$21.5^{+2.1}_{-1.7}$	$-0.04^{+0.17}_{-0.20}$	$49.1^{+5.2}_{-3.9}$	$0.66^{+0.08}_{-0.10}$	$2.2^{+0.5}_{-0.5}$	$3.3^{+0.6}_{-0.9} \times 10^{56}$	960^{+430}_{-410}	$0.19^{+0.07}_{-0.08}$	924	13.0
GW170608	$10.9^{+5.3}_{-1.7}$	$7.6^{+1.3}_{-2.1}$	$7.9^{+0.2}_{-0.2}$	$0.03^{+0.19}_{-0.07}$	$17.8^{+3.2}_{-0.7}$	$0.69^{+0.04}_{-0.04}$	$0.9^{+0.0}_{-0.1}$	$3.5^{+0.4}_{-1.3} \times 10^{56}$	320^{+120}_{-110}	$0.07^{+0.02}_{-0.02}$	396	14.9
GW170729	$50.6^{+16.6}_{-10.2}$	$34.3^{+9.1}_{-10.1}$	$35.7^{+6.5}_{-4.7}$	$0.36^{+0.21}_{-0.25}$	$80.3^{+14.6}_{-10.2}$	$0.81^{+0.07}_{-0.13}$	$4.8^{+1.7}_{-1.7}$	$4.2^{+0.9}_{-1.5} \times 10^{56}$	2750^{+1350}_{-1320}	$0.48^{+0.19}_{-0.20}$	1033	10.8
GW170809	$35.2^{+8.3}_{-6.0}$	$23.8^{+5.2}_{-5.1}$	$25.0^{+2.1}_{-1.6}$	$0.07^{+0.16}_{-0.16}$	$56.4^{+5.2}_{-3.7}$	$0.70^{+0.08}_{-0.09}$	$2.7^{+0.6}_{-0.6}$	$3.5^{+0.6}_{-0.9} \times 10^{56}$	990^{+320}_{-380}	$0.20^{+0.05}_{-0.07}$	340	12.4
GW170814	$30.7^{+5.7}_{-3.0}$	$25.3^{+2.9}_{-4.1}$	$24.2^{+1.4}_{-1.1}$	$0.07^{+0.12}_{-0.11}$	$53.4^{+3.2}_{-2.4}$	$0.72^{+0.07}_{-0.05}$	$2.7^{+0.4}_{-0.3}$	$3.7^{+0.4}_{-0.5} \times 10^{56}$	580^{+160}_{-210}	$0.12^{+0.03}_{-0.04}$	87	15.9
GW170817	$1.46^{+0.12}_{-0.10}$	$1.27^{+0.09}_{-0.09}$	$1.186^{+0.001}_{-0.001}$	$0.00^{+0.02}_{-0.01}$	≤ 2.8	≤ 0.89	≥ 0.04	$\geq 0.1 \times 10^{56}$	40^{+10}_{-10}	$0.01^{+0.00}_{-0.00}$	16	33.0
GW170818	$35.5^{+7.5}_{-4.7}$	$26.8^{+4.3}_{-5.2}$	$26.7^{+2.1}_{-1.7}$	$-0.09^{+0.18}_{-0.21}$	$59.8^{+4.8}_{-3.8}$	$0.67^{+0.07}_{-0.08}$	$2.7^{+0.5}_{-0.5}$	$3.4^{+0.5}_{-0.7} \times 10^{56}$	1020^{+430}_{-360}	$0.20^{+0.07}_{-0.07}$	39	11.3
GW170823	$39.6^{+10.0}_{-6.6}$	$29.4^{+6.3}_{-7.1}$	$29.3^{+4.2}_{-3.2}$	$0.08^{+0.20}_{-0.22}$	$65.6^{+9.4}_{-6.6}$	$0.71^{+0.08}_{-0.10}$	$3.3^{+0.9}_{-0.8}$	$3.6^{+0.6}_{-0.9} \times 10^{56}$	1850^{+840}_{-840}	$0.34^{+0.13}_{-0.14}$	1651	11.5

Now, 10 BH merger event data are publicly open.

arXiv:1811.12907

GraceDB — Gravitational-Wave Candidate Event Database

HOME | PUBLIC ALERTS | SEARCH | LATEST | DOCUMENTATION | LOGIN

Latest — as of 20 July 2019 05:57:05 UTC

Test and MDC events and superevents are not included in the search results by default; see the query help for information on how to search for events and superevents in those categories.

Query:

Search for: Superevent

Search

UID	Labels	t_start	t_0	t_end	FAR (Hz)	UTC Created
S190720a	ADVOK SKYMAP_READY EMBRIGHT_READY PASTRO_READY DQOK GCN_PRELIM_SENT	1247616533.703127	1247616534.704102	1247616535.860840	3.801e-09	2019-07-20 00:08:53 UTC
S190718y	ADVOK SKYMAP_READY EMBRIGHT_READY PASTRO_READY DQOK GCN_PRELIM_SENT	1247495729.067865	1247495730.067865	1247495731.067865	3.648e-08	2019-07-18 14:35:34 UTC
S190707q	PE_READY ADVOK SKYMAP_READY EMBRIGHT_READY PASTRO_READY DQOK GCN_PRELIM_SENT	1246527223.118398	1246527224.181226	1246527225.284180	5.265e-12	2019-07-07 09:33:44 UTC
S190706ai	PE_READY ADVOK SKYMAP_READY EMBRIGHT_READY PASTRO_READY DQOK GCN_PRELIM_SENT	1246487218.321541	1246487219.344727	1246487220.585938	1.901e-09	2019-07-06 22:26:57 UTC
S190701ah	PE_READY ADVOK SKYMAP_READY EMBRIGHT_READY PASTRO_READY DQOK GCN_PRELIM_SENT	1246048403.576563	1246048404.577637	1246048405.814941	1.916e-08	2019-07-01 20:33:24 UTC
S190630ag	PE_READY ADVOK SKYMAP_READY EMBRIGHT_READY PASTRO_READY DQOK GCN_PRELIM_SENT	1245955942.175325	1245955943.179550	1245955944.183184	1.435e-13	2019-06-30 18:52:28 UTC
S190602aq	PE_READY ADVOK SKYMAP_READY EMBRIGHT_READY PASTRO_READY DQOK GCN_PRELIM_SENT	1243533584.081266	1243533585.089355	1243533586.346191	1.901e-09	2019-06-02 17:59:51 UTC
S190524q	ADVNO SKYMAP_READY EMBRIGHT_READY PASTRO_READY DQOK GCN_PRELIM_SENT	1242708743.678669	1242708744.678669	1242708746.133301	6.971e-09	2019-05-24 04:52:30 UTC
S190521r	PE_READY ADVOK SKYMAP_READY EMBRIGHT_READY PASTRO_READY DQOK GCN_PRELIM_SENT	1242459856.453418	1242459857.460739	1242459858.642090	3.168e-10	2019-05-21 07:44:22 UTC
S190521g	PE_READY ADVOK SKYMAP_READY EMBRIGHT_READY PASTRO_READY DQOK GCN_PRELIM_SENT	1242442966.447266	1242442967.606934	1242442968.888184	3.801e-09	2019-05-21 03:02:49 UTC
S190519bj	PE_READY ADVOK SKYMAP_READY EMBRIGHT_READY PASTRO_READY DQOK GCN_PRELIM_SENT	1242315361.378873	1242315362.655762	1242315363.676270	5.702e-09	2019-05-19 15:36:04 UTC
S190518bb	ADVNO SKYMAP_READY EMBRIGHT_READY PASTRO_READY DQOK GCN_PRELIM_SENT	1242242376.474609	1242242377.474609	1242242380.922655	1.004e-08	2019-05-18 19:19:39 UTC
S190517h	PE_READY ADVOK SKYMAP_READY EMBRIGHT_READY PASTRO_READY DQOK GCN_PRELIM_SENT	1242107478.819517	1242107479.994141	1242107480.994141	2.373e-09	2019-05-17 05:51:23 UTC
S190513bm	PE_READY ADVOK SKYMAP_READY EMBRIGHT_READY PASTRO_READY DQOK GCN_PRELIM_SENT	1241816085.736106	1241816086.869141	1241816087.869141	3.734e-13	2019-05-13 20:54:48 UTC
S190512at	PE_READY ADVOK SKYMAP_READY EMBRIGHT_READY PASTRO_READY DQOK GCN_PRELIM_SENT	1241719651.411441	1241719652.416286	1241719653.518066	1.901e-09	2019-05-12 18:07:42 UTC
S190510g	ADVOK SKYMAP_READY EMBRIGHT_READY PASTRO_READY DQOK GCN_PRELIM_SENT	1241492396.291636	1241492397.291636	1241492398.293185	8.834e-09	2019-05-10 03:00:03 UTC
S190503bf	ADVOK SKYMAP_READY EMBRIGHT_READY PASTRO_READY DQOK GCN_PRELIM_SENT	1240944861.288574	1240944862.412598	1240944863.422852	1.636e-09	2019-05-03 18:54:26 UTC
S190426c	PE_READY ADVOK SKYMAP_READY EMBRIGHT_READY PASTRO_READY DQOK GCN_PRELIM_SENT	1240327332.331668	1240327333.348145	1240327334.353516	1.947e-08	2019-04-26 15:22:15 UTC
S190425z	ADVOK SKYMAP_READY EMBRIGHT_READY PASTRO_READY DQOK	1240215502.011549	1240215503.011549	1240215504.018242	4.538e-13	2019-04-25 08:18:26 UTC
S190421ar	PE_READY ADVOK SKYMAP_READY EMBRIGHT_READY PASTRO_READY DQOK GCN_PRELIM_SENT	1239917953.250977	1239917954.409180	1239917955.409180	1.489e-08	2019-04-21 21:39:16 UTC
S190412m	PE_READY ADVOK SKYMAP_READY EMBRIGHT_READY PASTRO_READY DQOK GCN_PRELIM_SENT	1239082261.146717	1239082262.222168	1239082263.229492	1.683e-27	2019-04-12 05:31:03 UTC
S190408an	PE_READY ADVOK SKYMAP_READY EMBRIGHT_READY PASTRO_READY DQOK GCN_PRELIM_SENT	1238782699.268296	1238782700.287958	1238782701.359863	2.811e-18	2019-04-08 18:18:27 UTC
S190405ar	ADVNO SKYMAP_READY EMBRIGHT_READY PASTRO_READY DQOK	1238515307.863646	1238515308.863646	1238515309.863646	2.141e-04	2019-04-05 16:01:56 UTC

LIGO/Virgo O3 has started last April, and KAGRA will join soon.

Test of GR using coalescing binaries

- Inspiral phase(large separation) (Cutler et al, PRL 70 2984(1993))

  Clean system: ~ point particles

  Accurate theoretical prediction of waveform is possible.

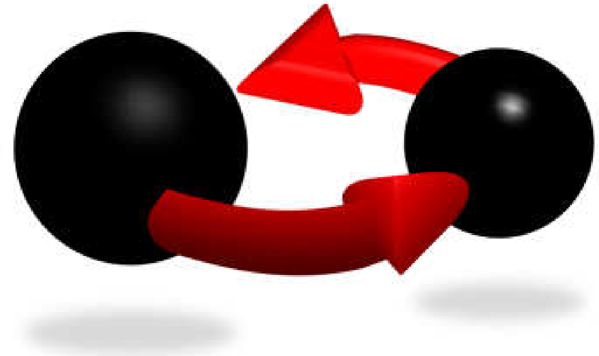

Waveform in Fourier space for quasi-circular inspiral

$$h(f) \approx A f^{-7/6} e^{i\Psi(f)}$$

$$A = \frac{1}{\sqrt{20\pi^3}} \frac{\mathcal{M}^{5/6}}{D_L}, \quad \mathcal{M} = \mu^{3/5} M^{2/5}, \quad \eta = \frac{\mu}{M}$$

$$\Psi = 2\pi f t_c - \varphi_c + \frac{3}{128}(\pi \mathcal{M} f)^{-5/3}\left[1 + \underbrace{\frac{20}{9}\left(\frac{743}{331} + \frac{11}{4}\eta\right) v^2}_{\text{1PN}} - \underbrace{(16\pi - \beta) v^3}_{\text{1.5PN}} + \cdots\right]$$

$$v^3 \equiv \pi M f$$

Parametrized test of gravitational wave form

$$h(f) \approx A f^{-7/6} e^{i\Psi(f)}$$

GW waveform from a binary in a quasi-circular orbit

$$\begin{cases} A(f) \rightarrow \left(1 + \sum_i \alpha_i u^{a_i}\right) A_{GR}(f) \\ \Psi(f) \rightarrow \Psi_{GR}(f) + \sum_i \beta_i u^{b_i} \end{cases}$$

Theory	a	α	b	β
Brans-Dicke [9, 10, 14–16]	–	0	-7/3	β
Parity-Violation [22, 34–37]	1	α	0	–
Variable $G(t)$ [38]	-8/3	α	-13/3	β
Massive Graviton [8–14]	–	0	-1	β
Quadratic Curvature [23, 44]	–	0	-1/3	β
Extra Dimensions [45]	–	0	-13/3	β
Dynamical Chern-Simons [46]	+3	α	+4/3	β

(Yunes & Pretorius (2009))

Calculable leading order corrections are described by the parameter b and β in many cases.

Parametrized Post Einstein (PPE) formalism

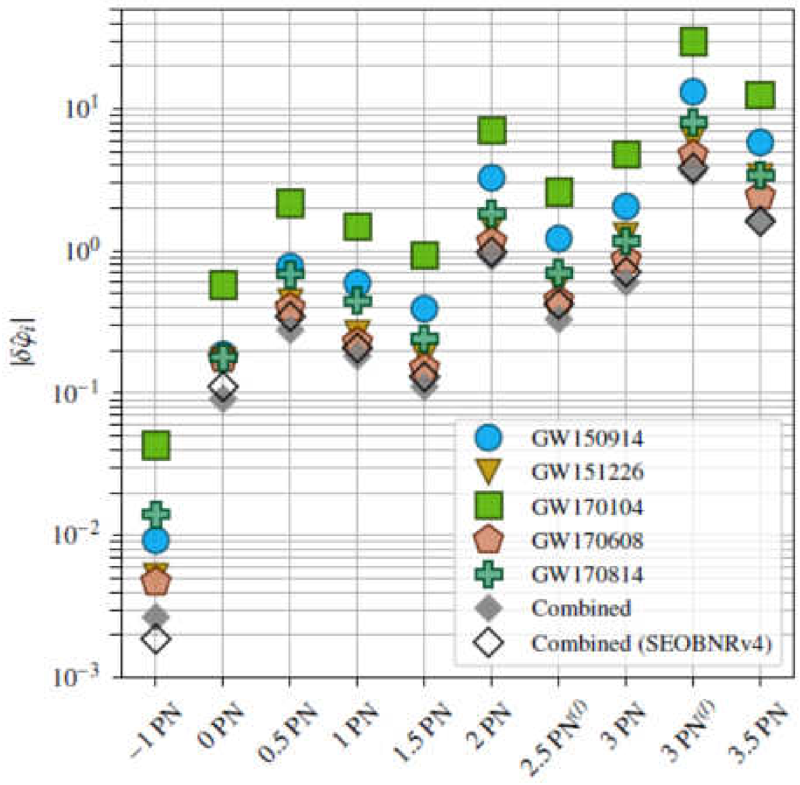

(LIGO/Virgo 1903.04467)

Constraint on the relative amplitude of deviation from GR for each PN coefficient of the phase evolution

This is a constraint on generation of gravitational waves in the inspiral phase.

The leading tidal effects appear at 5PN order

But this is not the whole story.
There are also many examples of possible extension from GR that go beyond the scope of PPE formalism.

Is the parametrized test sufficient?

Ex.1) Massive scalar dipole radiation

Scalar-tensor theory is already strongly constrained by the pulsar timing observations.

Constraint on dipole radiation from GW170817 (1811.00364)

$$B \leq 1.2 \times 10^{-5}$$

is to be compared with pulsar constraint

$$|B| \lesssim 6 \times 10^{-8}$$

However, the scalar field may have a small mass.

The scalar field should be stabilized for $T_{\rm univ}$<10MeV, since the effective gravitational coupling G_N must be unchanged during BBN.

$$\Rightarrow \quad m_{\rm scalar} > 10^{-16}\,{\rm eV},$$

which is marginally sufficient to evade the constraint from pulsar timing (PSR J0348+0432).

LIGO-Virgo-KAGRA band corresponds to the mass range

$$10^{-13}\,{\rm eV} > m_{\rm scalar} > 10^{-14}\,{\rm eV}$$ (Ramazanoglu et al. 1601.07475)

In this case, it is easy to obtain the leading post-Newtonian correction.

At low frequencies there is no scalar emission and the fifth force is suppressed at a distance beyond its Compton wavelength.

There is a mass parameter region in which the dipole radiation occurs only at around the binary coalescence.

$$\phi \sim Y_{lm}(\Omega) h_l^{(1)}(kr) \int d^3x\, e^{-i\omega(t-t')} (kr)^l Y_{lm}^*(\Omega) S(x') \qquad \omega^2 = k^2 + m^2$$

$$T_{rt}^{(\phi)} \sim \phi_{,r}\phi_{,t} \sim k\omega\phi\phi$$: energy flux

For the energy loss rate due to the dipole radiation ($l = 1$), we will have an extra factor $k^3/\omega^3 \theta(\omega - m)$ to the energy flux, compared with the massless case.

However, it is not so easy to obtain the full waveform covering the merger-ringdown phase.

Result of application of the test to the real data

K. Yamada, T. Narikawa and TT arXiv:1905.11859

$$\left(\frac{dE}{dt}\right)_d = A\left(\frac{dE}{dt}\right)_Q \frac{k^3}{\omega^3}\Theta(\omega^2 - m^2)(2\pi f M)^{-2/3}$$

90% confidence level upper bound

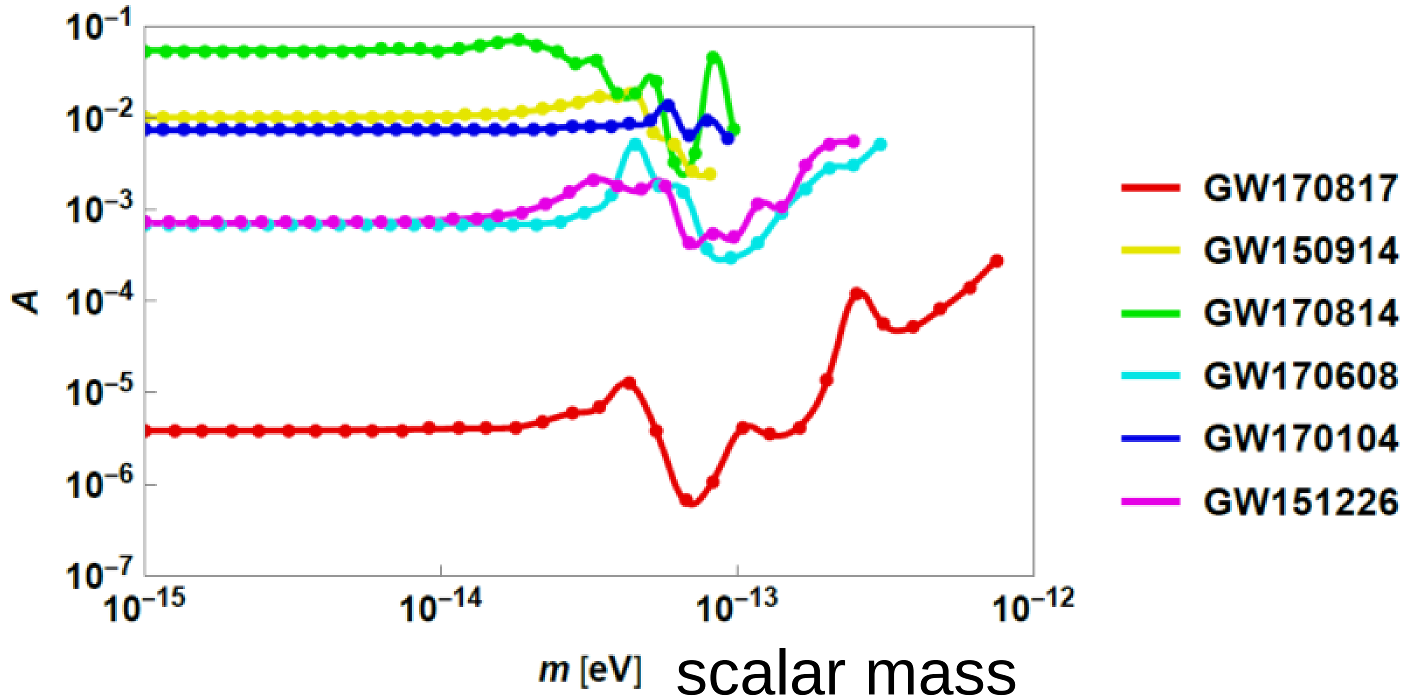

scalar mass

Even we introduce the scalar mass, GR is more preferred.

Einstein dilaton Gauss-Bonnet

$$S \supset \frac{\alpha_{EdGB}}{G_N}\int d^4x\sqrt{-g}\,\theta\left(R^2-4R_{\mu\nu}R^{\mu\nu}+R^{\alpha\beta}{}_{\mu\nu}R^{\mu\nu}{}_{\alpha\beta}\right)$$
$$-\frac{1}{2G_N}\int d^4x\sqrt{-g}\left[(\partial\theta)^2-m^2\theta^2\right]$$

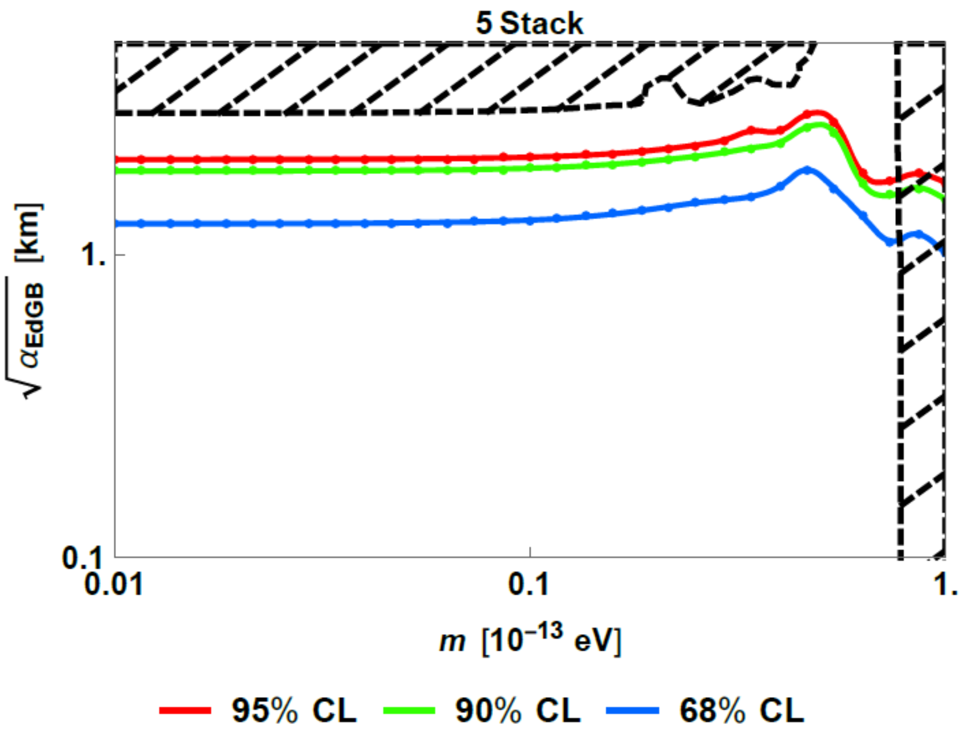

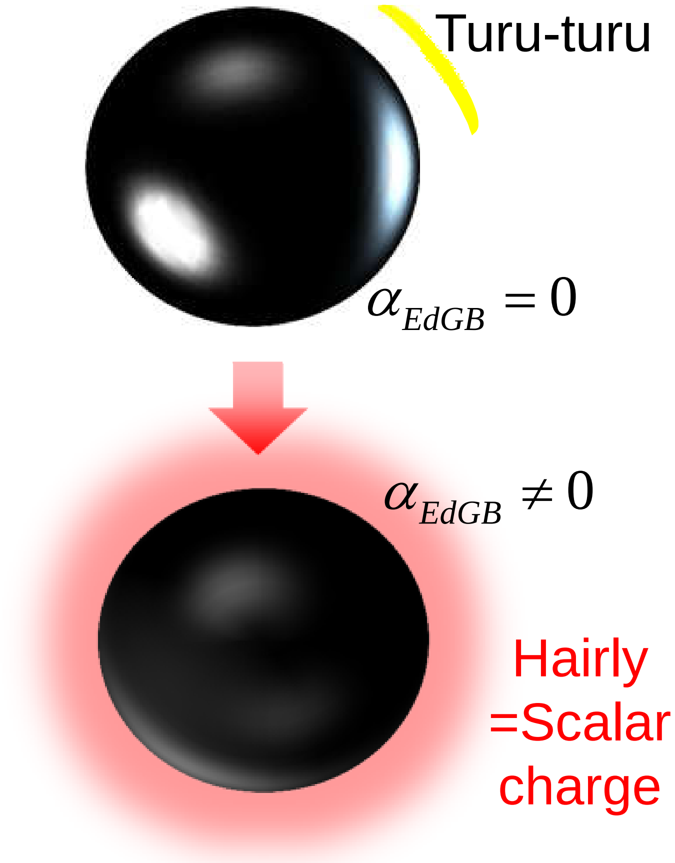

Gauss-Bonnet coupling with massive scalar field in this mass range was constrained for the first time.

Full waveform generation

- We want to use the merger-ringdown phase to give tighter constraint.
- However, the practical calculation of the waveform for modified gravity is limited to PN expansion.
- Iterative construction of solution is going to be developed. （Okounkova et al. 1911.02588)

For the precise determination of the phase evolution, something like renormalization group method may be required.

Gamma ray association with binary neutron star merger event GW170817

(arXiv:1710.05834)

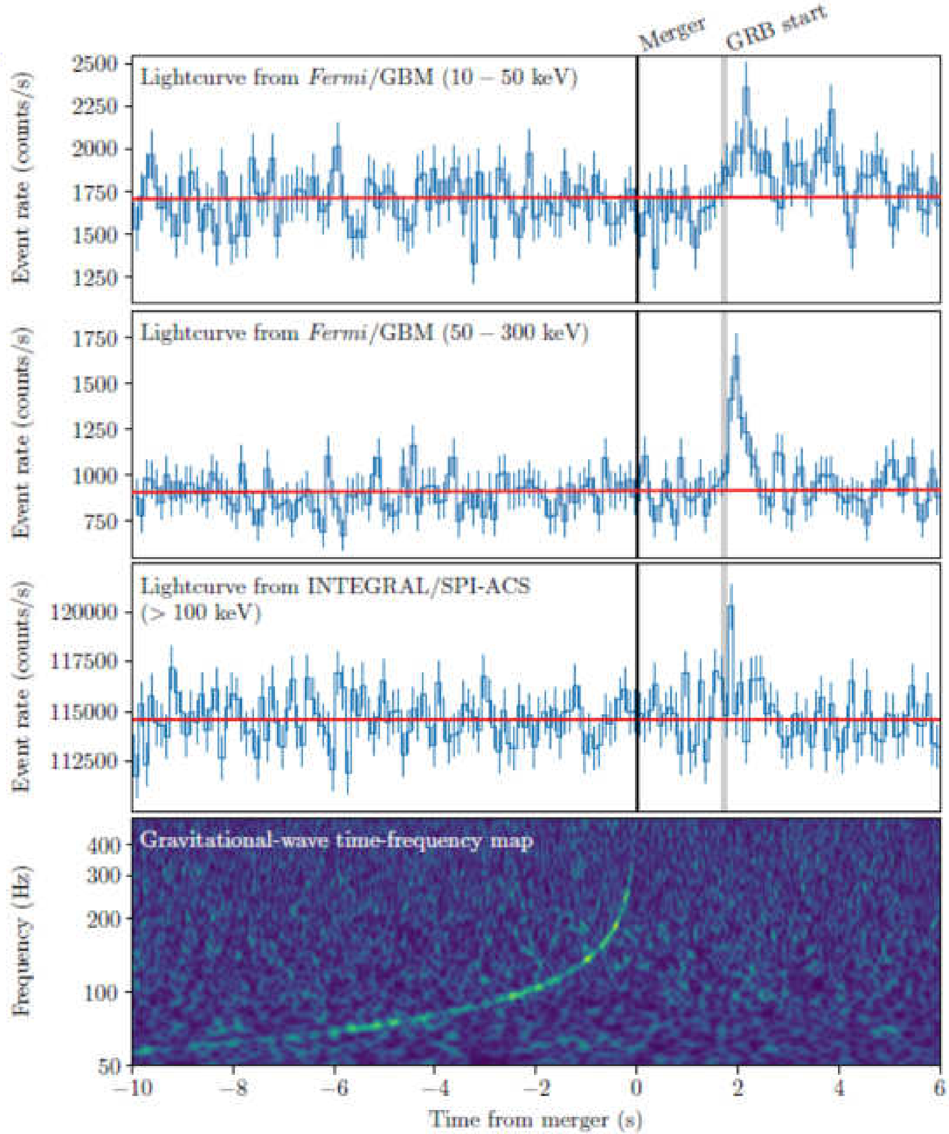

Propagation speed of gravitational waves

1.7sec delay of gamma ray detection over 40Mpc implies

$$\left|c_{GW}^2 - c_\gamma^2\right| < 10^{-15}$$

Extension of gravity theory is tightly constrained.

Ex.) Horndeski theory: scalar-tensor theory with a single scalar field with only upto 2nd order time derivatives in EoM.

$$\mathcal{L}_2 = K(\phi, X),$$

$$\mathcal{L}_3 = -G_3(\phi, X)\Box\phi$$

$$\mathcal{L}_4 = G_4(\phi, X)R + G_{4X}\left[(\Box\phi)^2 - (\nabla_\mu\nabla_\nu\phi)^2\right],$$

$$\mathcal{L}_5 = G_5(\phi, X)G_{\mu\nu}\nabla^\mu\nabla^\nu\phi - \frac{G_{5X}}{6}\left[(\Box\phi)^3 - 3(\Box\phi)(\nabla_\mu\nabla_\nu\phi)^2 + 2(\nabla_\mu\nabla_\nu\phi)^3\right]$$

$$c_{gw}^2 = \frac{G_4 - X\left(\ddot{\phi}G_{5,X} + G_{5,\phi}\right)}{G_4 - 2XG_{4,X} - X\left(H\dot{\phi}G_{5,X} - G_{5,\phi}\right)}$$

$$\Rightarrow \quad G_4 = G_4(\phi),\ G_5 = 0$$

Only rather traditional models survive.

K-essence, DGP braneworld, scalar-tensor theory

Ex.2 Parity violating dispersion relation

Modified dispersion relation of GWs
has been tested by LIGO/Virgo collaboration. (1903.04467)

$$\delta\Phi_\alpha(f) = \mathrm{sign}(A_\alpha)\begin{cases} \dfrac{\pi D_L}{\alpha-1}\lambda_{A,\mathrm{eff}}^{\alpha-2}\left(\dfrac{f}{c}\right)^{\alpha-1}, & \alpha \neq 1 \\ \dfrac{\pi D_L}{\lambda_{A,\mathrm{eff}}}\ln\left(\dfrac{\pi G \mathcal{M}^{\mathrm{det}} f}{c^3}\right), & \alpha = 1 \end{cases}$$

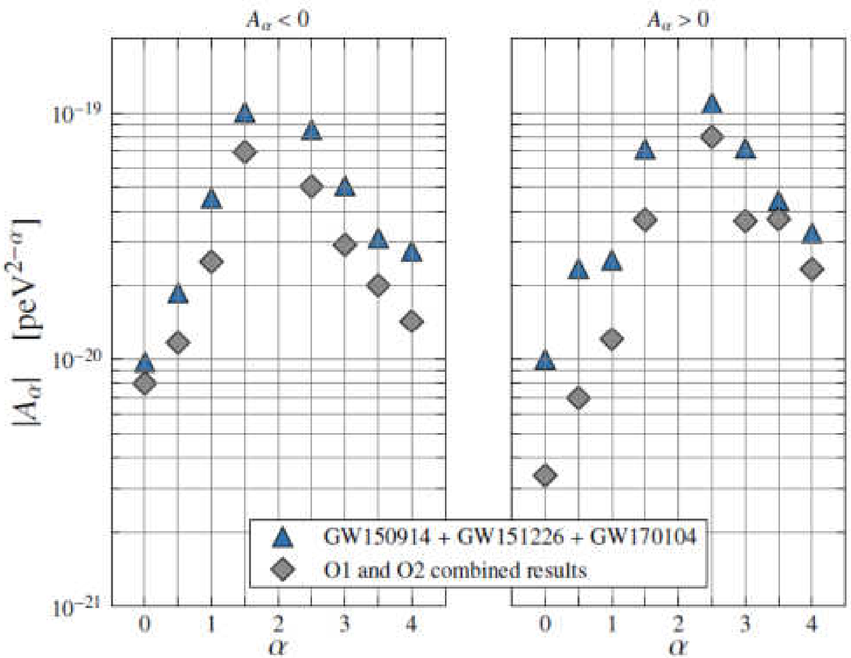

α=0 ($A_\alpha > 0$) corresponds to the graviton mass
(although non-covariant theory)
$\Rightarrow \quad m_{\mathrm{graviton}} < 4.7 \times 10^{-23}$ eV

How about the parity violating cases?
Right and left handed gravitons propagate differently.

$$\mathbf{h}^{(L,R)} = \frac{1}{\sqrt{2}}\left(\mathbf{h}^{(+)} + i\mathbf{h}^{(\times)}\right)$$

Generalized action including a term with the factor

$\varepsilon^{\alpha\beta\mu\nu} R_{\alpha\beta\gamma\delta} R_{\mu\nu\rho\sigma}$ and a scalar field.

$\phi \varepsilon^{\alpha\beta\mu\nu} R_{\alpha\beta\gamma\delta} R_{\mu\nu}{}^{\gamma\delta}$: Chern-Simons gravity is a typical example

Quadratic action (Nishizawa, Kobayashi 1809.00815)

$$L_{PV} = \frac{1}{4}\left[\gamma(t) \varepsilon^{ijk} \dot{h}_{il}\, \partial_j \dot{h}_k{}^l + \frac{\delta(t)}{a^2(t)} \varepsilon^{ijk} \partial^2 h_{il}\, \partial_j h_k{}^l \right]$$

Action for the Chern-Simons: $\gamma(t) = \delta(t)$

$$\sqrt{-g}\left(L_{GR} + L_{PV}\right) = a^2(t)\left[1 - k\lambda_{L,R}\gamma(t)\right]\left[h'^2_{L,R} - k^2 h^2_{L,R}\right]$$

Large modification of amplitude occurs when this factor change in time: $a(t)\sqrt{1 - k\lambda_{L,R}\gamma(t)}\, h_{L,R} \sim \text{const.}$

Remark) At a slightly higher frequency, negative energy states appear.

In more general models dispersion relation becomes

$$\omega^2 + \left(2aH - \lambda_{L,R} k \gamma'\right) i\omega - \left(1 + \lambda_{L,R} k (\gamma - \delta)\right) k^2 \approx 0$$

In general, gravitational wave phase is also modified.

Subtle difference from PPE case

$$h_{L,R} = \frac{1}{\sqrt{2}}\left(h_+ \pm i h_\times\right)$$

$$\Rightarrow \quad h_{L,R}^{\text{mod}}(f) = e^{i\delta\Phi_{L,R}} h_{L,R}(f)$$

$$\Rightarrow \quad h_+^{\text{mod}} = \frac{1}{\sqrt{2}}\left(h_L^{\text{mod}} + h_R^{\text{mod}}\right) = \frac{1}{2}\left(e^{i\delta\Phi_L} + e^{i\delta\Phi_R}\right)h_+ + \frac{1}{2i}\left(e^{i\delta\Phi_L} - e^{i\delta\Phi_R}\right)h_\times$$

$$h_\times^{\text{mod}} = \frac{1}{\sqrt{2}i}\left(h_L^{\text{mod}} - h_R^{\text{mod}}\right) = \frac{1}{2i}\left(e^{i\delta\Phi_L} - e^{i\delta\Phi_R}\right)h_+ + \frac{1}{2}\left(e^{i\delta\Phi_L} + e^{i\delta\Phi_R}\right)h_\times$$

$$\Rightarrow \quad h_{obs}^{\text{mod}} = A_+ h_+^{\text{mod}} + A_\times h_\times^{\text{mod}}$$

PPE case: $\delta\Phi_L(f) = \delta\Phi_R(f) = \delta\Phi_L(-f) = \delta\Phi_R(-f)$

PV case: $\delta\Phi_L(f) = -\delta\Phi_R(f) = -\delta\Phi_L(-f) = \delta\Phi_R(-f)$

In case of face-on in-spiral, h_L and h_R are dominated by positive and negative frequency components, respectively.

Then PV is degenerate with PPE.

➡ It is important to determine the binary inclination angle using multi-GW detector or multi-messenger information is important.

Result of application of the test to the real data

$$\Psi(f) \rightarrow \Psi_{GR}(f) + \lambda_{L,R} \sum_i \beta_i u^{b_i}$$

(K. Yamada and TT in preparation)

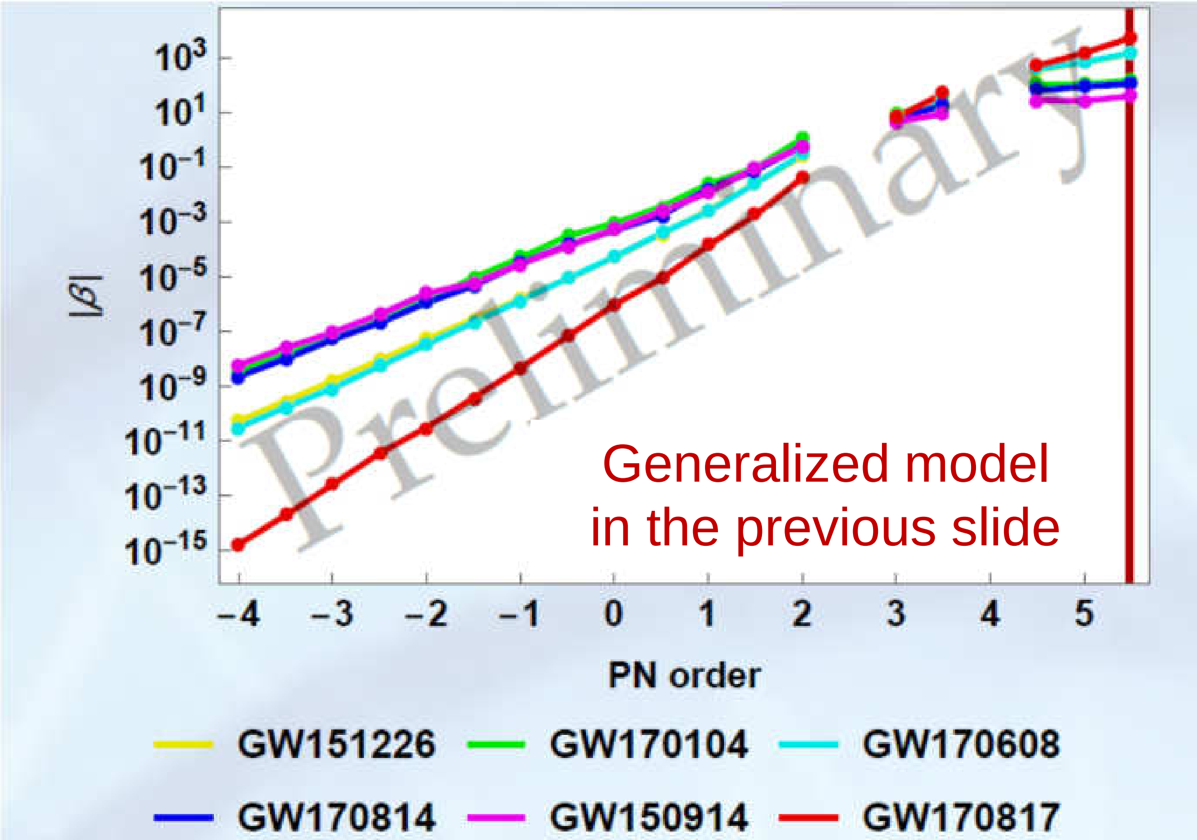

The obtained upper bound magnitude is similar to non-parity violating case.

$|\gamma - \delta| < 10^{-11} km$ → $|\gamma - \delta| < 10^{-18} km$

Constraint from $|c_T - 1| < 10^{-15}$
(Nishizawa, Kobayashi 1809.00815)

Modified propagation is easy to predict?

- We do not have to treat the merger ringdown phase separately.
- However, waveform can be quite complicated due to environmental uncertainties.

Ex.) Bigravity (De Felice et al, JCAP 1406 (2014) 037)

Phase shifts of two graviton propagation modes

$$\delta\Phi_{1,2} = -\int dx \frac{\mu\sqrt{c-1}}{2\sqrt{2y}}\left(1+y \mp \sqrt{1+2y\frac{1-\alpha}{1+\alpha}+y^2}\right)$$

$$\sqrt{c-1} \approx \mu^{-1}\sqrt{3(1+\alpha)\rho} \qquad y = \frac{2\omega^2(c-1)}{\mu^2}$$

The phase shifts depend on the matter energy density ρ on the line of sight.

The frequencies where the modification becomes large also depend on the matter energy density.

Black Hole Echoes

There is a claim that echoes might have been detected in the LIGO GW events.

(Abedi et al, arXiv:1612.00266)

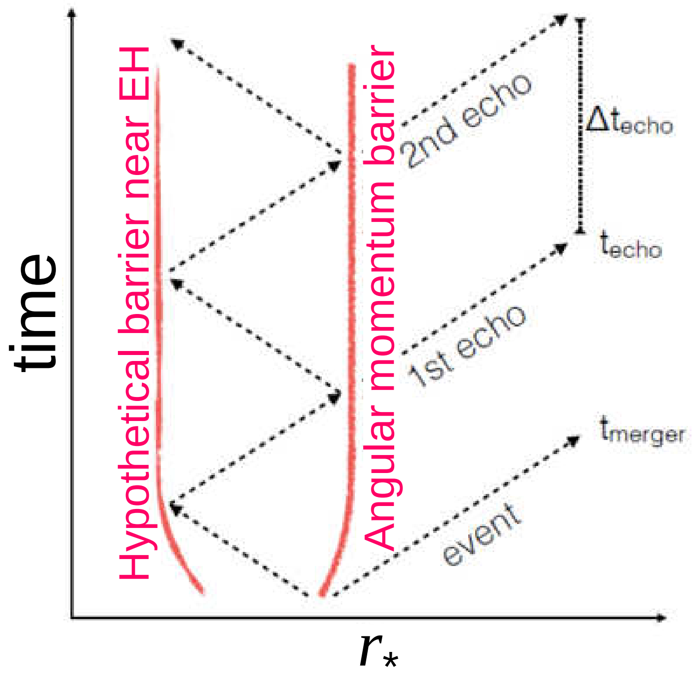

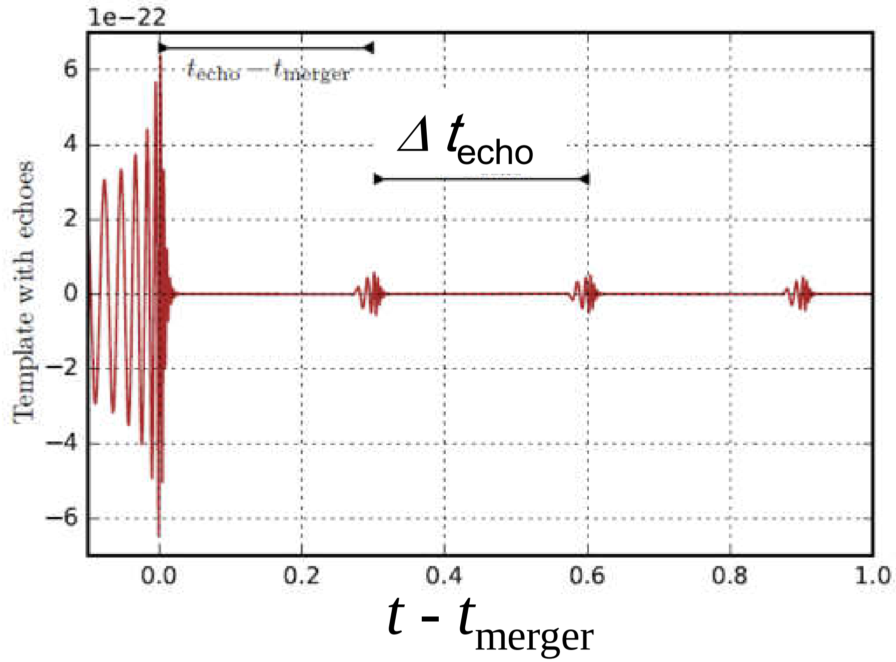

1) Reflecting boundary at the Planck distance from the horizon
2) Slowly decaying echoes of the same waveform with overall phase shift π.
3) Echo period Δt_{echo} is the one predicted by the angular mom. barrier and the reflection wall at the Planck distance from the horizon.

   $\rightarrow 3\sigma$ detection of signal

We considered more appropriate template will increase the significance (arXiv:1704.07175)

Perturbation Equation of Kerr BH (Sasaki-Nakamura) [$l=m=2$ mode only]

$$\frac{d^2Y}{dr_*^2}+V_{SN}Y=0 \quad \Rightarrow \quad Y=\begin{cases}\exp(-i\omega r_*) & (r_*\to\infty)\\ Y_{up}\exp(-ikr_*)+Y_{down}\exp(ikr_*) & (r_*\to-\infty)\end{cases}$$

Reflection rate :

$$\sqrt{R(f)}=\sqrt{C}\,\frac{|Y_{up}|}{|Y_{down}|}$$

$C\neq 1$ since V_{SN} is not real

Phase shift :

$$\phi(f)=\arg\left(\frac{Y_{up}}{Y_{down}}\right)?$$

depends on the frequency f.

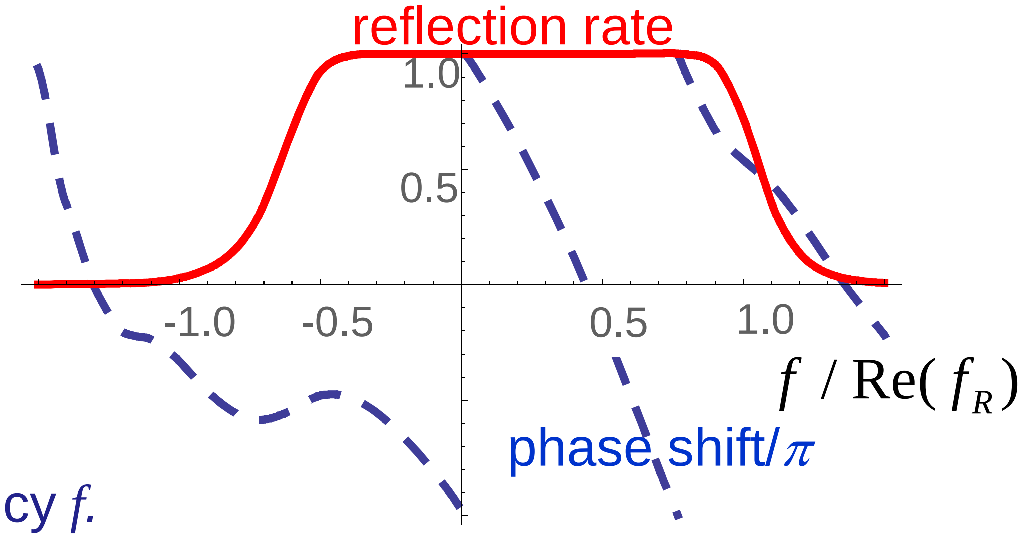

ϕ can depend on the nature of the near-horizon boundary even if we assume complete reflection.

However, $\phi(f)$ can be approximated by a linear fn. for a narrow range of f close to the QNM frequency f_R.

⇒ $\phi(f)$ can be absorbed by the time interval between echoes and the overall phase shift ϕ_0

Power spectrum changes at each reflection

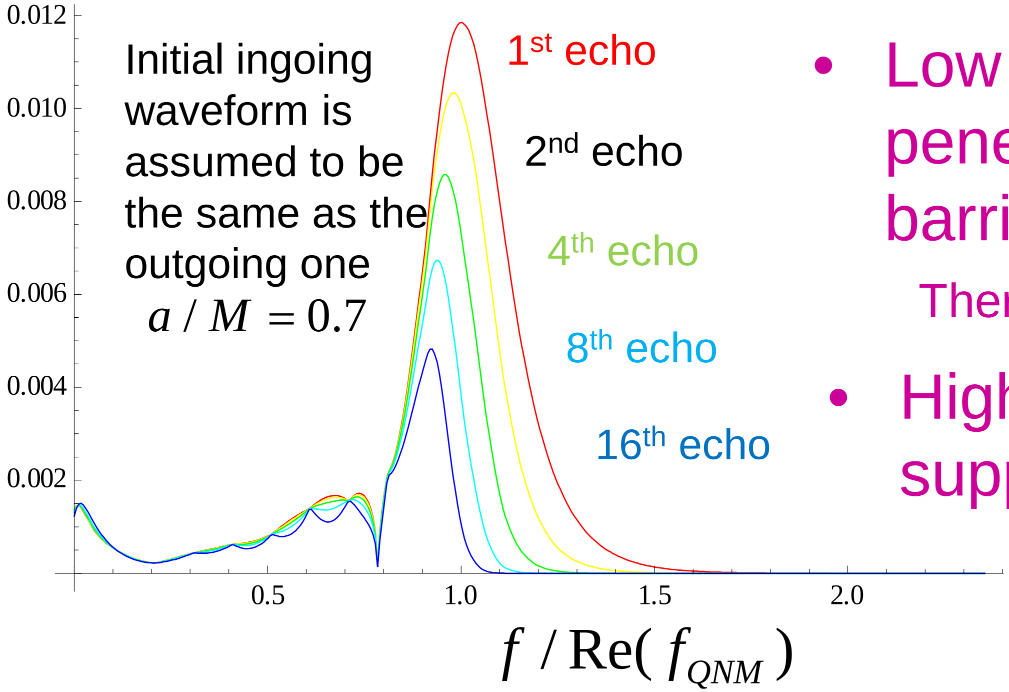

- Low frequency modes cannot penetrate the angular momentum barrier.

  There is a different opinion (1907.03091)

- Higher frequency modes are suppressed at later time.

How does the significance of the echo signal change by taking into account this more physically motivated waveform?

N. Uchikata, H. Nakano, T. Narikawa, N. Sago, H. Tagoshi, TT arXiv:1906.00838

Analysis method

We follow the basic strategy taken by Abedi et al. (2017)

Search the maximum signal-to-noise ratio (SNR) in the interval of $0.99 \leq x \leq 1.01$, varying the other parameters.

$$x \equiv \frac{t_{echo}}{\Delta t_{echo}}$$

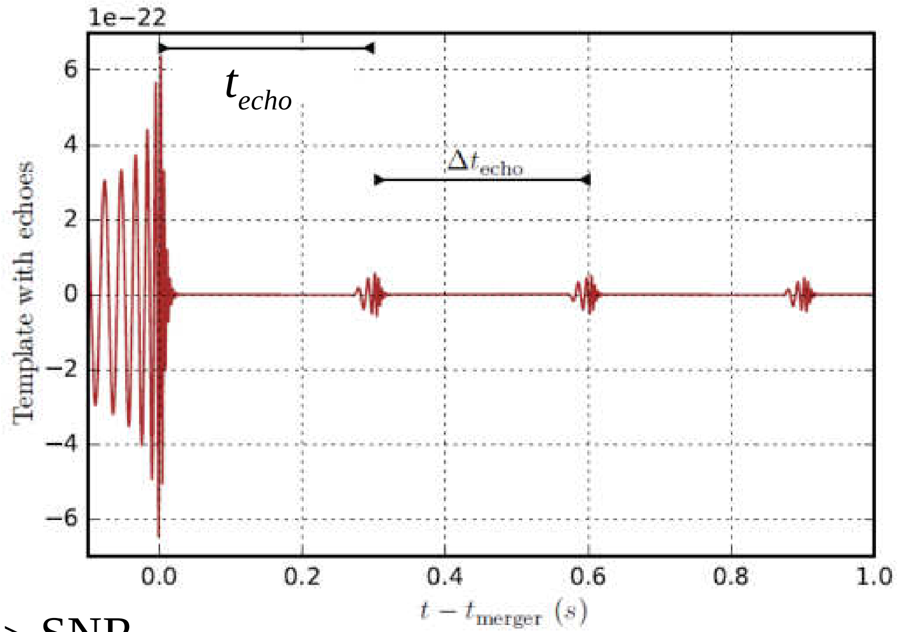

Background estimation

Perform the same analysis for the neighboring 4096sec data, where no signal is expected.

p-value

$$p \equiv \frac{\#\text{of reference data with SNR} > \text{SNR}_{\text{event}}}{\#\text{of all reference data}}$$

If we find $p << 1$, there might be some true signal.

Results of our re-analysis

We performed reanalysis using our new template, which we think is more physically motivated, expecting the increase of significance.

List of p-values

	Simple repetition	Our template
GW150914	0.157	0.984
GW151012	0.047	0.882
GW170104	0.071	0.677
GW170608	0.079	0.488
GW170729	0.567	0.575
GW170814	0.024	0.472
GW170818	0.929	0.976
GW170823	0.055	0.315
average	0.241	0.671

2.75σ

The analysis using the template assuming simple repetition of the same waveform gives relatively small p-value, although p-value is large for a few events.

Expected improvement of the significance was not achieved.

Which frequency contributes to the match for the best fit parameters?

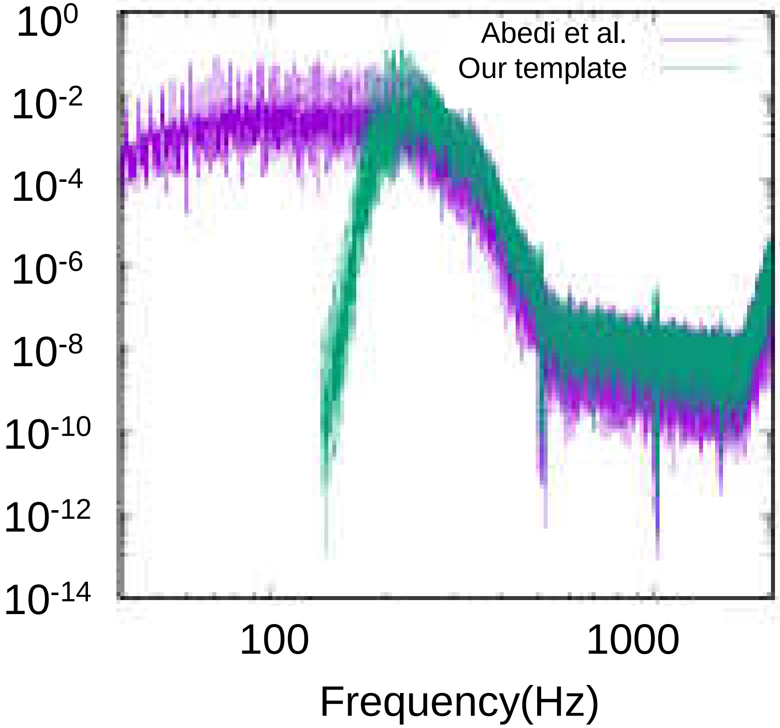

As expected, low frequency modes contribute a lot in the case of the original template.

We evaluate the echo spectrum excited by a small particle falling into Kerr black hole, as a mimicker of binary coalescence.

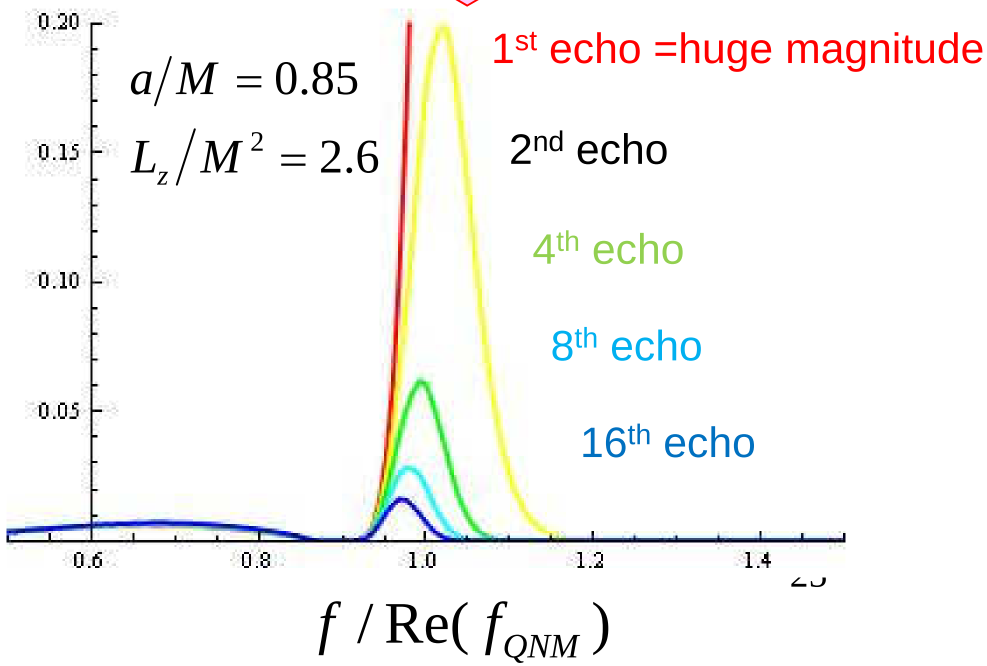

- As expected, the low frequency modes are suppressed.
- Early phase of echo can be much louder.

Summary

Gravitational wave observations opened up a new window for modified gravity.

There are many ideas that can escape un-directed test of GR, such as massive field radiation, echoes and so on.

More aspects that can be tested by the ground GW detector network, to which KAGRA will join soon, will be remaining to be uncovered.

Dedicated data analyses are to be implemented.

For this purpose, more theoretical studies are definitely necessary.